Sustainable Energy & Fuels

ROYAL SOCIETY OF CHEMISTRY

PAPER

View Article Online
View Journal | View Issue



Cite this: *Sustainable Energy Fuels*, 2025, **9**, 5018

# A vanillin bio-based redox polymer as a cathode material for lithium organic batteries†

Tijs Lap,[a] Gabriele Lingua,[a] Daniele Mantione[ab] and David Mecerreyes *[ab]

Organic materials such as redox polymers have gained much attention as sustainable electrode materials for the next generation of batteries. Specifically, biomass-derived materials are intriguing due to their potential for their integration into a circular economy. Here we demonstrate a facile one-step polymerization reaction of vanillin, industrially produced by lignin-fueled biorefineries, which provides a bio-based catechol redox polymer. The insoluble poly(vanillin) is synthesized during a one-pot, acid-catalyzed polymerization reaction of vanillin in which auto-polycondensation, methyl-deprotection and crosslinking occur simultaneously. The electrochemical performance of poly(vanillin) was assessed as a cathode material in Li half-cells using either 1.0 M $LiPF_6$ in EC : DEC (1 : 1, v/v) or 1.0 M LiTFSI in DOL : DME (1 : 1, v/v) as the electrolyte. The latter displayed the best performance for poly(vanillin), with specific capacities of up to 101.25 mAh $g^{-1}$ and a capacity retention of 85.5% after 350 cycles. The d*Q*/d*V* plot exposes a well-defined reversible catechol redox at 3.2 V (*vs.* $Li/Li^+$). Furthermore, the use of water as the processing solvent for electrode fabrication using a poly(ionic liquid) as the binder was demonstrated. This work shows a scalable synthetic route to a bio-based catechol redox polymer from vanillin to be used as a high-voltage organic electrode material.

Received 7th March 2025
Accepted 23rd July 2025

DOI: 10.1039/d5se00349k

rsc.li/sustainable-energy



## Introduction

Bio-based polymers are made from renewable biomass and have a reduced footprint and natural degradability, making them interesting for a green and circular economy.[1,2] For their syntheses, raw materials like plant oils, fatty acids, cellulose and lignin are often used. Of these, the latter, lignin, is the main biomass feedstock for high-value aromatic chemicals.[3–5] Moreover, lignin availability is potentially enormous both directly from biomass as well as from paper industry waste streams.[6–8] It is due to this gigantic availability that much effort has been put in utilizing the lignin polymer directly in copolymers or composites, while lignin depolymerization methods for bio refineries are explored to yield high-value aromatics.[4,9–13] Although multiple compounds like ferulic acid, guaiacol, dopamine and vanillin can be derived from lignin, currently only vanillin is produced from lignin at industrial levels, underlining its status as an important renewable aromatic building block.[4,14,15]

The recognition of the abundance and usefulness of vanillin by the food industry is demonstrated by its employment as a main flavoring and fragrance agent with an annual demand of 20 thousand tons. Interestingly, in recent years efforts have been made to exploit vanillin for the design of new monomers and polymers. Caillol *et al.*[16] reported on multiple epoxy thermosets, while Cramail and co-workers demonstrated the use of vanillin for concrete plasticizers, aromatic polyesters or polyazomethines.[16–23] More recently, vanillin-based non-isocyanate polyurethanes have been proposed as sustainable alternatives for rigid and soft foams, as well as for coatings, adhesives, sealants, elastomers and biomedical applications.[24–27]

A sector that could profit extensively from bio-based polymers is the battery industry.[28–30] With the current surge in battery demand, many electrode materials (*e.g.* cobalt, manganese and nickel) are troubled by predictions of scarcity, topographical limited harvesting, and vast footprints related to their processing.[31] However, over the last decade, redox-active polymers, used as organic electrode materials (OEMs), have displayed great promise as sustainable alternatives.[32] Specifically, those obtainable from biomass are interesting due to the possible harvesting without topographical restrictions and their renewable feedstock, making their production fossil fuels independent.[33] With this incentive, several attempts have been made to incorporate vanillin-based polymers as electrode materials in batteries.[34,35] The latter can be realized by a facile oxidation of the vanillin molecule, generating the electroactive benzoquinone scaffold, or *via* methyl-deprotection which gives rise to the catechol redox moiety.[36] Although several vanillin-based polymers utilizing the benzoquinone redox center display promising stability and

[a]*POLYMAT, University of the Basque Country UPV/EHU, Joxe Mari Korta Center, 20018, Donostia-San Sebastiań, Spain. E-mail: david.mecerreyes@ehu.es; Tel: +34 943 018018*

[b]*Ikerbasque, Basque Foundation for Science, 48013 Bilbao, Spain*

† Electronic supplementary information (ESI) available. See DOI: https://doi.org/10.1039/d5se00349k

capacities, they are outperformed by those utilizing the catechol moiety, since the latter exhibits a large theoretical capacity of up to 402.57 mAh $g^{-1}$ and high discharge potentials of 3.2–3.4 V (*vs.* $Li/Li^+$).[37,38]

Indeed, several catechol redox polymers, either bio-based or bio-inspired, have displayed excellent performances. For example, the bio-derived poly(dopamine) displayed a good specific capacity of up to 133 mAh $g^{-1}$ for Li-ion batteries when coated on few-walled carbon nanotubes.[39] Moreover, Nagaraj Patil *et al.* impressively improved this specific capacity with $\approx$100 mAh $g^{-1}$ by synthesizing the bio-inspired poly(4-vinyl catechol), eliminating significant amounts of unnecessary mass.[38] Unfortunately, the dopamine availability from natural resources is limited and poly(4-vinyl catechol) is not bio-based while the latter also requires a multi-step synthesis.[40] This makes catechol redox polymers derived from the widely available bio-vanillin a more than welcome alternative.

To use vanillin for the synthesis of catechol redox polymers, Liedel *et al.* reported on a multi-step synthesis of vanillin-functionalized chitosan and bisvanillonitrile biopolymers as catechol electrode materials, displaying limited specific capacities of 80 and 55 mAh $g^{-1}$ after 100 cycles, respectively.[41,42] Although interesting, the current literature suggests that high-performance bio-based catechol redox polymers derived from abundant biomass, like vanillin, utilizing a facile and scalable synthesis are a very welcome addition for organic electrode materials.

Therefore, in this work, we report a scalable, facile, quantitative, one-step polymerization reaction for vanillin and its reference molecule protocatechuic aldehyde, providing a pathway towards industrially producible, bio-based poly(-catechol) materials. Note that protocatechuic aldehyde, which can only be obtained from bio resources such as cocoa beans, hemp and red sage in small amounts, was used as a reference material as large-scale preparation is impeded by its limited availability.[43] The reported synthesis circumvents cumbersome multi-step syntheses, by being multifunctional, as the polycondensation, methyl-deprotection and crosslinking occur simultaneously, delivering a catechol polymer derived from vanillin. To examine the electrochemical performance, both polymers were subjected to cyclic voltammetry (CV) and Li half-cell cycling as cathodes. We also demonstrate the possible compatibility of the poly(catechols) with water-processable binders for the fabrication of electrodes with even further enhanced sustainability.

# Experimental

### Materials and equipment

Sulfuric acid (95.0–98.0%, ACS reagent) was purchased from Thermo Fisher Scientific. Toluene, vanillin (ReagentPlus, 99%®), polystyrene-*block*-poly(ethylene-ranbutylene)-*block*-polystyrene (SEBS, average $M_w$ ~118 000 by GPC, contains >0.03% antioxidant as the inhibitor), 1,3-dioxolane and 1,2-dimethoxyethane (DME) were purchased from Sigma-Aldrich. 3,4-Dihydroxybenzaldehyde (98%) was purchased from BDL PHARMATECH GmbH. Poly(diallyldimethylammonium)-dibutyl hydrogen phosphate was synthesized previously.[44] Lithium bis(trifluoromethanesulfonyl)imide (LiTFSI) was purchased from Iolitec. Battery electrolyte (1.0 M lithium hexafluorophosphate in ethylene carbonate/diethyl carbonate, 1 : 1, v/v) was purchased from Solvionic. Carbon coated aluminum foil (width 260 mm, thickness 20 μm), lithium metal (width 60 mm, thickness 100 μm) and conductive carbon black super C65 (Timical) were purchased from Gelon Energy Co. Limited. The 1.0 M LiTFSI DOL : DME electrolyte and SEBS stock solutions (15 wt% in toluene) were prepared overnight before use. All other chemicals and solvents were used as received.

### SEM images

The scanning electron microscopy (SEM) images and energy-dispersive X-ray spectroscopy (EDS) mappings of the samples were obtained using a TM3030 series Hitachi Tabletop Microscope, as shown in ESI-II-4.†

### Electrochemical testing

Cyclic voltammetry of the vanillin, protocatechuic aldehyde or their polymers was performed in a Li half-cell. Li half-cells, based on cathodes of poly(vanillin) or poly(protocatechuic aldehyde), were assembled inside an argon-filled glovebox. For detailed descriptions of electrode formulations, Li half-cell setups and employed electrolytes see ESI-I-2.†

### Synthesis of poly(vanillin)

10 g (65.73 mmol) of vanillin was dissolved in 20 mL of conc. $H_2SO_4$. The reaction mixture was stirred at 130 °C for 5–15 hours. The solidified reaction mixture was added to 300 mL of demineralized water. Subsequently, the polymer was repeatedly submerged in 200 mL demineralized water until no colored monomer solution was obtained anymore. Finally, the polymer was dried overnight under vacuum at 60 °C. Yield: 96%. ATR-FTIR ($cm^{-1}$): 3043, 2554, 1584, 1506, 1456, 1270, 1200, 1146, 1029, 862, 614.

### Synthesis of poly(protocatechuic aldehyde)

1 g (7.24 mmol) of protocatechuic aldehyde was dissolved in 2 mL of conc. $H_2SO_4$. The reaction mixture was stirred at 130 °C for 5–15 hours. The solidified reaction mixture was added to 300 mL of demineralized water. Subsequently, the polymer was repeatedly submerged in 200 mL demineralized water until no colored monomer solution was obtained anymore. Finally, the polymer was dried overnight under vacuum at 60 °C. Yield: 97%. ATR-FTIR ($cm^{-1}$): 3071, 2941, 2525, 1559, 1507, 1442, 1270, 1136, 1088, 1026, 856, 617.

# Results and discussion

### Synthesis and characterization of poly(vanillin) and poly(protocatechuic aldehyde)

Two bio-based polymers were synthesized as organic electrode materials, employing the same facile method. The design of a simplistic and scalable polymerization process delivering

quantitative yields was key to fully exploit the large-scale commercial availability of bio-vanillin, and to provide a potentially interesting process for industry to produce high-performance vanillin-based electrode materials. Moreover, before vanillin could be utilized as an electrode material, a demethylation was required to generate the redox-active catechol moiety. While this type of reaction generally includes the use of harsh reagents like $BBr_3$, some studies observed a methyl deprotection reaction while using conditions similar to those reported in this work, potentially paving the way for a possible *in situ* demethylation of the vanillin substructure during the polycondensation polymerization reaction.[45] To confirm that our vanillin system will pass through the suggested pathway, a polymer analogue already containing the catechol redox center was synthesized as the reference material: poly(protocatechuic aldehyde). This polymer served as a reference for both the chemical and electrochemical characterization of poly(vanillin). Even though protocatechuic aldehyde already contains the catechol moiety and is obtainable from biomass, its limited bio-availability makes it less appealing for large-scale industrial processes.

The established polymerization reaction is depicted in Scheme 1a, and is composed of a facile, quantitative and scalable one-step polycondensation reaction yielding poly(vanillin) and poly(protocatechuic aldehyde), using concentrated sulfuric acid both as the solvent and Brønsted acid catalyst for the

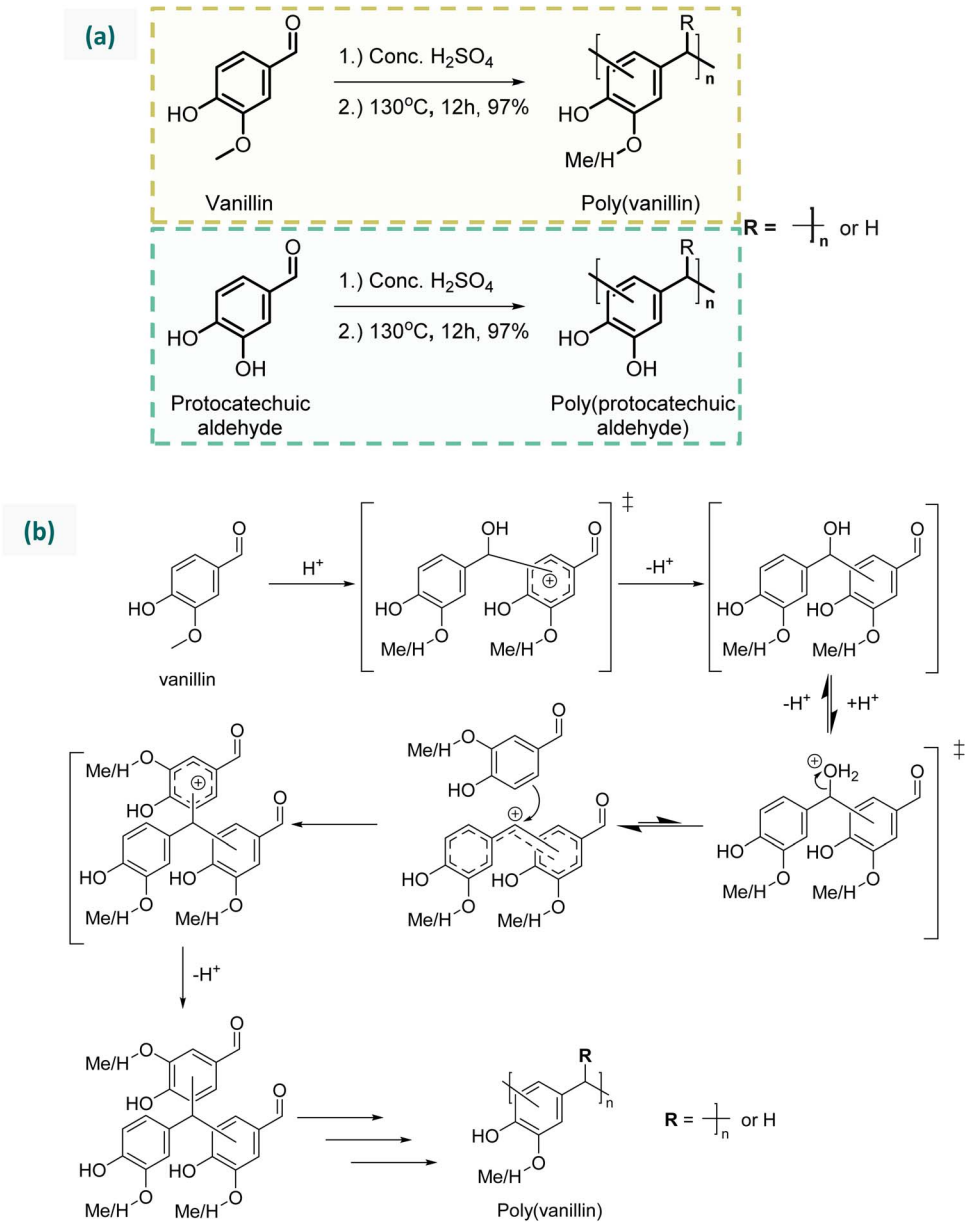


Scheme 1 The (a) one-step, quantitative polycondensation of (top) vanillin and (bottom) protocatechuic aldehyde in conc. $H_2SO_4$, yielding poly(vanillin) and poly(protocatechuic aldehyde), respectively. And (b) the anticipated reaction mechanism of the condensation polymerization of vanillin, inspired on mechanistical studies.

 

Friedel–Crafts alkylation.[46–48] Like the polymerization step, the workup is simple, merely including a washing step utilizing only water.

The optimized reaction conditions shown in Scheme 1a were found after careful screening of various reaction temperatures (room temperature, 50, 70, 90 and 130 °C), as well as the concentrations of vanillin and of $H_2SO_4$. Lower reaction temperatures demanded longer reaction times, while reducing the concentration of vanillin lowered the conversion, since a notable difference in yield and product solubility was observed. The latter was also observed for more diluted $H_2SO_4$ reaction systems.

To the best of our knowledge, this is the first time that both vanillin and protocatechuic aldehyde are polymerized in this manner, albeit being inspired by previous work and the presence of mechanistic studies for similar reactions in the

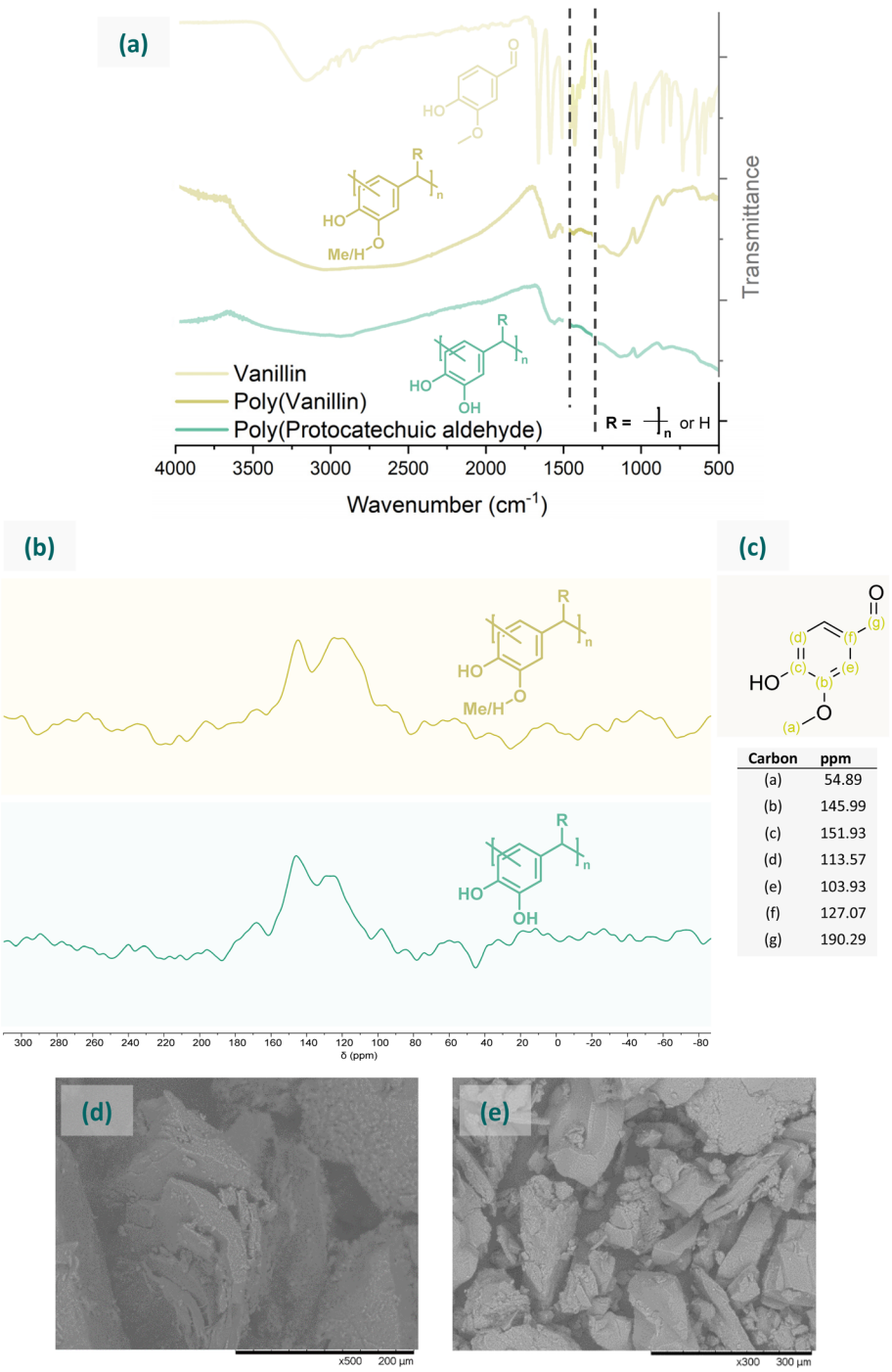


Fig. 1 The (a) ATR-FTIR spectra of vanillin, poly(vanillin) and poly(protocatechuic aldehyde), and the (b) stacked $^{13}C$ solid-state NMR spectra of poly(vanillin) and poly(protocatechuic aldehyde), with (c) the reported chemical shifts (ppm) of vanillin obtained by $^{13}C$ solid-state NMR.[56] The SEM images of poly(vanillin) and poly(protocatechuic aldehyde) are shown with a magnification of (d) 500× and (e) 300×, respectively.

literature.[49,50] The anticipated mechanism for the synthesis of poly(vanillin) is shown in Scheme 1b and is similar for protocatechuic aldehyde. Here, the concentrated $H_2SO_4$ activates the aldehyde moiety by protonation, inviting the aromatic scaffolds to perform a nucleophilic attack on the carbonyl, connecting the aromatic monomers.

The stacked $^1$H NMR spectra depicted in ESI-II-1† show the $^1$H NMR spectrum of vanillin and the soluble fraction of the final product which was mostly insoluble. An NMR sample of assumingly oligomers was obtained upon stirring the final polymeric product in DMSO-$d_6$ for 24 hours at elevated temperatures, followed by filtration. The obtained $^1$H NMR spectrum reveals that this Friedel–Craft reaction is not site-specific and addition to any of the three available aromatic positions is arbitrary. Three signals for the methoxy group of vanillin with different chemical shifts ($\delta$: 3.79, 3.84 and 3.87 ppm) appear, as well as numerous new aromatic signals with slightly different chemical shifts ($\delta$: 6.8–7.5 ppm), indicating that the addition happens in a random fashion. The presence of 4 reactive sites in both monomers indeed results in a cross-linked polymeric material, which could help to counteract dissolution of the active material into the electrolyte.[51] Moreover, the material was easily dispersed in multiple casting solvents (*e.g.* toluene, NMP, water) with no visible solubility, offering a vast range of choices for processing solvents for the electrode fabrication. However, in contrast, the cross-linked nature of the products impeded both NMR and GPC analyses of the polymeric materials, despite attempts to perform them. Therefore, ATR-FTIR, $^{13}$C solid-state NMR (SS NMR) and scanning electrode microscopy (SEM) studies were performed.

Fig. 1a shows the stacked ATR-FTIR spectra of vanillin, poly(vanillin) and poly(protocatechuic aldehyde), whereas the ATR-FTIR spectra of protocatechuic aldehyde and poly(-protocatechuic aldehyde) are compared in ESI-II-2.† While comparing the spectra of vanillin and its polymer analogue, several observations indicate the successful polymerization. First, broader peaks with lower intensities can be observed for poly(vanillin) with respect to those of the monomer. This indicates an increase in intramolecular hydrogen bonding between the different hydroxyl groups, as well as the presence of a range of different vibrational energies for the C–H vibrations, which result from the chemical anisotropy within the polymer.[52] Second, the hydroxyl peak (3155 $cm^{-1}$ = O–H, stretching) remains present in the polymeric material, while the strong C=O stretching signal at 1661 $cm^{-1}$ related to the aldehyde of the small molecule disappears completely upon polymerization. Finally, the C–H vibrations of the $CH_3$- and CHO group of vanillin at the respective wavenumbers of 2945–3021 and 2858 $cm^{-1}$ are not visible anymore for poly(vanillin).[53,54] However, the presence of the $CH_3$ group in the final polymeric structure cannot be excluded based on ATR-FTIR alone, since the moderate signal could be overlapped by the broader hydroxyl vibrations. Other techniques, like SS NMR and half-cell cycling, can confirm the presence or absence of the methyl moiety. However, when comparing the spectra of poly(vanillin) and poly(protocatechuic aldehyde) in Fig. 1a, the ATR-FTIR spectra of both polymers appear to be identical. Only a minor difference can be observed from wavenumber 2863 to 2943 $cm^{-1}$, where C–H vibrations corresponding to non-crosslinked methylene sites can be observed for poly(-protocatechuic aldehyde).[55]

To confirm the aforementioned demethylation and to further characterize and compare the structures of both synthesized polymers, $^{13}$C solid-state NMR was performed. The stacked spectra of poly(vanillin) and poly(protocatechuic aldehyde) are depicted in Fig. 1b, while the chemical shifts of vanillin, as reported in the literature, are shown in Fig. 1c.[56] Focusing on the spectrum corresponding to poly(vanillin) first, it becomes clear that no methoxy-related signal ($\delta \approx 54.89$ ppm) is present in the spectrum of poly(vanillin). This supports the hypothesis that the deprotection of the hydroxyl occurs during polymerization. Second, no peak corresponding to the aldehyde carbon ($\delta \approx 190.29$ ppm) can be observed, indicating the consumption of the aldehyde functionality during the polycondensation reaction. From the obtained SS NMR spectra, neither a full conversion from the aldehyde to a methylene bridge, nor the partial conversion to a hydroxyl can be confirmed, since corresponding peaks are not visible. However, assuming the full conversion seems justified based on the strongly acidic conditions and the high temperature used. The presence of the conc. $H_2SO_4$ will result in the protonation of the hydroxyl intermediate, pushing the reaction to completion, driven by the generation of water as the leaving group. Thirdly, in the spectrum of poly(vanillin) two distinct signals can be observed and assigned to either the aromatic carbons ($\delta$ = 100–130 ppm) or the carbons adjacent to the hydroxyl groups ($\delta$ = 135–160 ppm). Both are in strong agreement with the values listed in Fig. 1c. Finally, when comparing the spectrum of poly(vanillin) with that of the reference polymer, poly(-protocatechuic aldehyde), both appear to be very similar. Only negligible differences in the width of the aromatic signals can be noted. Indeed, the high degree of likeliness of these spectra confirms that the deprotection of the hydroxy group occurs in parallel with the polymerization reaction. Hence the polymerization of vanillin and protocatechuic aldehyde yields the same poly(catechol). However, for reasons of clarity, the poly(-catechol) obtained from vanillin will be addressed as poly(-vanillin) while the one obtained from protocatechuic aldehyde will be referred to as poly(protocatechuic aldehyde).

Altogether, this procedure enables the large-scale transformation of the industrially produced bio-vanillin into a bio-based catechol redox polymer with known impressive characteristics such as a high redox potential of 3.2–3.4 V (*vs.* $Li/Li^+$) and a theoretical capacity of 402.57 mAh $g^{-1}$.[38] Ultimately, SEM was used to visualize the morphology of the black polymer powders, as shown in Fig. 1d and e.

## Electrochemical characterization of poly(vanillin) and poly(protocatechuic aldehyde)

The electrochemical performances of vanillin, protocatechuic aldehyde and their polymer counterparts were assessed as cathodic materials by means of galvanostatic cycling (GC) and cycling voltammetry (CV) in Li-metal cells, using 1.0 M $LiPF_6$ in

 

ethylene carbonate (EC) : diethyl carbonate (DEC) (1 : 1, v/v) and 1.0 M LiTFSI in dioxolane (DOL) : dimethoxyethane (DME) (1 : 1, v/v) as electrolytes and [Act. Mat: $C_{65}$ : SEBS] = [40 : 50 : 10] as the electrode formulation. The produced electrodes had an active material loading of 0.92–1.8 mg cm$^{-2}$. First, the electrochemical features of the redox-active small molecules were investigated using CV and GC techniques. Both protocatechuic aldehyde and vanillin display poor cyclability, as reported in ESI-III-1–4.† The limited stability of the molecules is mainly related to their high solubility in organic electrolytes. In contrast, the cycling data for both poly(protocatechuic aldehyde) and poly(vanillin), shown in ESI-III-5–8† and Fig. 3 respectively, display the positive effect of polymerization on the electrochemical stability.

Fig. 2a and b show the d$Q$/d$V$ plots resulting from the galvanostatic cycling of the poly(vanillin)-based organic electrodes for the two different electrolytes at room temperature. The 1st, 5th and 75th cycles were selected, since the activation phase of the 1.0 M $LiPF_6$ in EC : DEC (1 : 1, v/v) containing cell was only completed after 70 cycles, as also becomes evident from Fig. 2c. Compared to the EC : DEC-based electrolyte, a better compatibility between the electrode and the DOL : DME-electrolyte can be observed from the d$Q$/d$V$ plot shown in Fig. 2a, where a more defined catechol oxidation and reduction peak appears at 3.2 V (*vs.* Li/Li$^+$) after a brief activation phase.[38] The swift appearance of the catechol redox couple and the more defined profile indicate the improved compatibility of this specific electrode formulation with the DOL : DME-based electrolyte, with respect to the carbonate-based commercial one. Furthermore, the appearance of the catechol redox profile additionally proves that the demethylation reaction of the vanillin scaffold and polymerization occur simultaneously.

The specific capacities over 350 cycles resulting from the galvanostatic cycling of the same Li half-cells are shown in Fig. 2c. The use of the commercial 1.0 M $LiPF_6$ in EC : DEC (1 : 1,

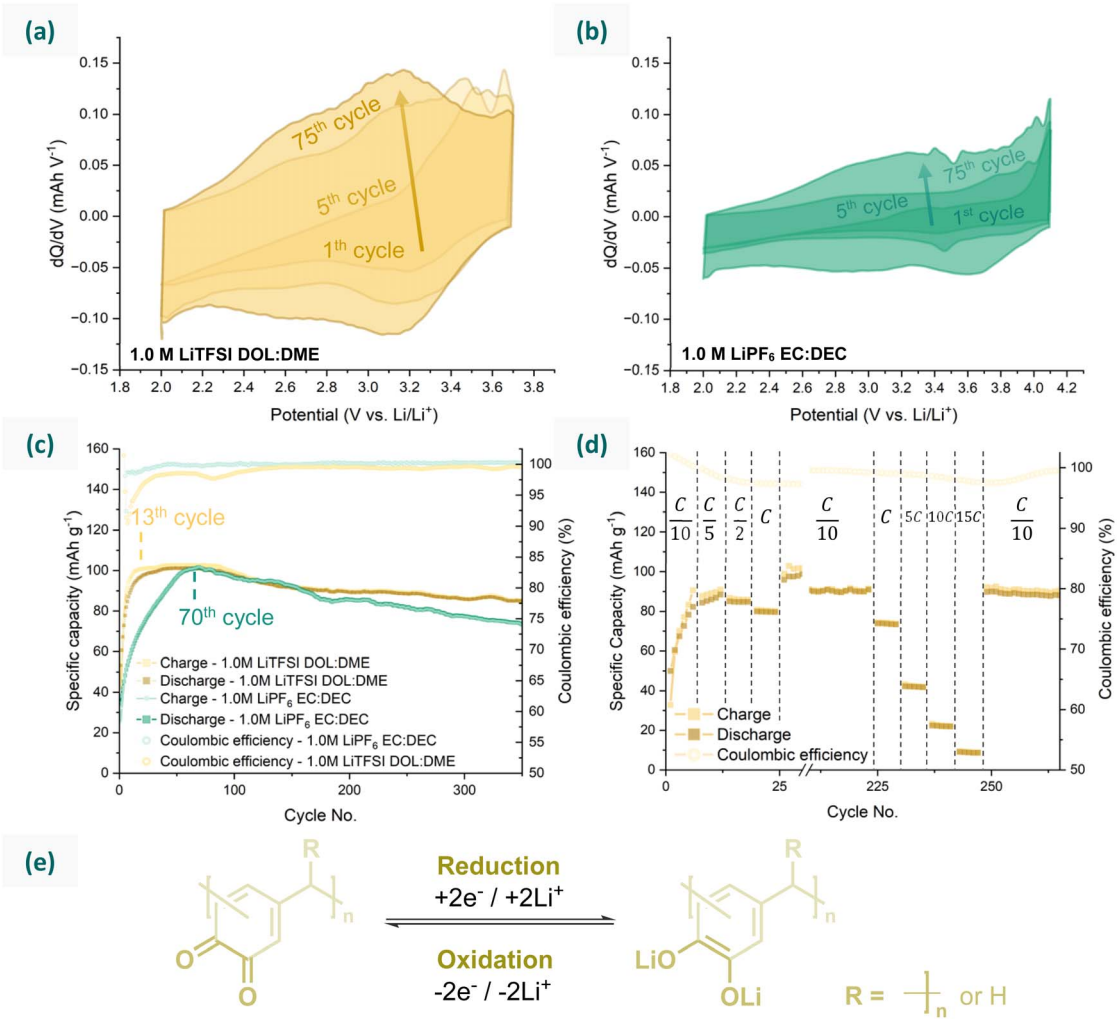


Fig. 2 The d$Q$/d$V$ plots of the 1st, 5th and 75th cycles of Li half-cells employing poly(vanillin) as the redox-active cathode material, utilizing [Act. Mat. : $C_{65}$ : SEBS] = [40 : 50 : 10] as the electrode formulation and either (a) 1.0 M LiTFSI in DOL : DME (1 : 1, v/v) or (b) 1.0 M $LiPF_6$ in EC : DEC (1 : 1, v/v) as the electrolyte and a C-rate of 0.1C. (c) The charge and discharge capacity as well as the correlating coulombic efficiency over 350 cycles for the same Li half-cells, utilizing either 1.0 M $LiPF_6$ in EC : DEC (1 : 1, v/v) (green) or 1.0 M LiTFSI in DOL : DME (1 : 1, v/v) (yellow) as the electrolyte and a C-rate of 0.1C. The C-rate test for a poly(vanillin) containing Li half-cell employing 1.0 M LiTFSI in DOL : DME (1 : 1, v/v) as the electrolyte is shown in (d), while (e) exhibits the anticipated electrochemical mechanism of the synthesized poly(catechol).

v/v) enabled the attainment of a satisfactory specific capacity output (101.71 mAh $g^{-1}$ after 70 cycles) and a capacity retention of 72.1% after 280 cycles at 0.1C. However, the poor impregnation by the electrolyte, as well as the low compatibility between the electrolyte and the electrode caused very long activation times (70 cycles) and poorly defined redox peaks (see Fig. 2b). A significant improvement was observed when switching to 1.0 M LiTFSI in DOL : DME (1 : 1, v/v) as the electrolyte. Fig. 2c shows that the activation period is greatly reduced to 13 cycles, along with capacity retention improvements from 72.1% to 85.5% after 280 cycles subsequent to reaching the peak specific capacity. Moreover, the peak specific capacity value of 101.25 mAh $g^{-1}$ is similar to the one observed with the commercial electrolyte.

Fig. 2d shows the rate capability assessment of poly(vanillin) combined with 1.0 M LiTFSI in DOL : DME (1 : 1, v/v) as the electrolyte. The Li-metal cell was subjected to a subsequent charging and discharging process at different C-rates (0.2, 0.5 and 1.0C) for 5 cycles each. The specific capacity of poly(vanillin) demonstrates decent resilience against the different applied currents of up to 1.0C, displaying values of 86.2, 84.8 and 79.8 mAh $g^{-1}$ for 0.2, 0.5 and 1.0C, respectively. For this reason, as well as for testing the capacity response to high currents, a second C-rate test was performed with the same cell after 200 cycles at 0.1C. Here, specific capacities of 73.7, 42.0, 22.2 and 8.8 mAh $g^{-1}$ were observed for C-rates of respectively 1.0, 5.0, 10.0 and 15.0C. Remarkably, a minor specific capacity fade of 13% (from 104.52 mAh $g^{-1}$ to 90.93 mAh $g^{-1}$) was observed after more than 200 cycles of repetitive charging and discharging, involving high C-rates currents, up to 15C. The limited specific capacity outputs at high C-rates can be imputed to the cross-linked nature of the polymer which results in a non-negligible internal resistance, thus restricting the ion movement and coordination process. Nonetheless, the rate performance of poly(vanillin) matches those of PDA reported by Patil *et al.* for electrodes with similar mass loading.[38] This together with the specific capacity recovery subsequent to the C-rate test with both moderate and high currents, the cycling stability and displayed specific capacity outputs show the great potential of this easy-to-synthesize biopolymer as the cathode material for batteries. In ESI-III-9,† for several C-rates, the obtained specific capacities are compared to values reported in the literature for both bio-inspired and bio-based catechol-bearing redox polymers.

The anticipated electrochemical mechanism of poly(catechol) is depicted in Fig. 2e. Here, the catechol moiety exhibits the well-known reversible two electron process resulting in either the oxidized *o*-quinone or reduced lithiated-catechol state.[38] For more detailed studies on the catechol electrochemistry, the reader is referred to other studies, as the literature on this is plentiful and mechanistical studies are beyond the scope of this paper.

Lastly, changes in electrode morphology were briefly investigated by SEM, as shown in ESI-III-10.† However, no changes were observed when comparing fresh electrodes to electrodes in either the fully charged or discharged state. Note that the latter electrodes were obtained after completing the activation phase.

To amplify the green character of the protocatechuic aldehyde and vanillin biopolymers, focus was shifted to the electrode fabrication process. Although the utilized electrode preparation method is robust, fast and does not involve high drying temperatures, SEBS requires the use of organic solvents, toluene in specific. Therefore, to circumvent the use of the latter as the casting solvent, the compatibility of poly(vanillin) and poly(protocatechuic aldehyde) with waterborne binders such as poly(diallyldimethylammonium) phosphate (PDADMA) poly(ionic liquid)s was explored. Two PDADMA-based poly(ionic liquid)s, using either dibutyl hydrogen phosphate (DBP) or diethyl hydrogen phosphate (DEP) as the counter-ion, were synthesized as reported previously and tested as water-soluble binders for the fabrication of bio-based water soluble organic electrodes.[44] The electrochemical performance of their fabricated electrodes was assessed with both 1.0 M LiTFSI in DOL : DME (1 : 1, v/v) and 1.0 M $LiPF_6$ in EC : DEC (1 : 1, v/v) electrolytes in Li half-cells.

The cycling performances of the PDADMA-DEP-based electrodes for both poly(vanillin) and poly(protocatechuic aldehyde) are shown in ESI-III-11.† Likewise, the cycling data of the PDADMA-DBP electrodes tested with 1.0 M LiTFSI DOL : DME (1 : 1, v/v) are depicted in ESI-III-12,† while the electrochemical performance of the PDADMA-DBP electrodes tested with the 1.0 M $LiPF_6$ EC : DEC (1 : 1, v/v) electrolyte is visualized in Fig. 3a for both polymers.

The PDADMA-DBP-based electrodes undoubtedly outperformed those based on PDADMA-DEP. Although the PDADMA-DEP electrodes displayed good cycling stability for poly(protocatechuic aldehyde) upon completion of the activation phase, the specific capacities remained low (see ESI-III-11†). In contrast, PDADMA-DBP containing electrodes display acceptable specific capacities with maximum values of 75 and 90 mAh $g^{-1}$ respectively for poly(protocatechuic aldehyde) and poly(vanillin), as reported in Fig. 3a. Surprisingly, under similar conditions in terms of binder and electrolytes, the poly(vanillin)-based electrode shows limited capacity outputs and rapid fading in comparison with the poly(protocatechuic aldehyde)-based one. However, similar results were obtained twice for this Li half-cell setup. Interestingly, here the Li half-cell containing poly(protocatechuic aldehyde), PDADMA-DBP as the binder and the $LiPF_6$-based electrolyte showed stable cycling along with specific capacity values of $\approx$78 mAh $g^{-1}$ after 350 cycles at 0.1C, with a coulombic efficiency approaching 100% (see Fig. 3a). The compatibility between the active material, binder and electrolyte proved to be a multi-variable problem. Although interesting, no further investigations were performed to understand the poor performance of some combinations of the PDADMA-binder, biopolymer and electrolyte, since this is beyond the scope of this study.

On the other hand, comparing the best performing half-cell configuration containing PDADMA-DBP with one that only differs by binder is of interest. Therefore, in Fig. 3b–d, the electrochemical performances of poly(protocatechuic aldehyde) with either PDADMA-DBP or SEBS as the binder and 1.0 M $LiPF_6$ EC : DEC (1 : 1, v/v) as the electrolyte were compared. In Fig. 3b the coulombic efficiencies and the charge–discharge capacities

 

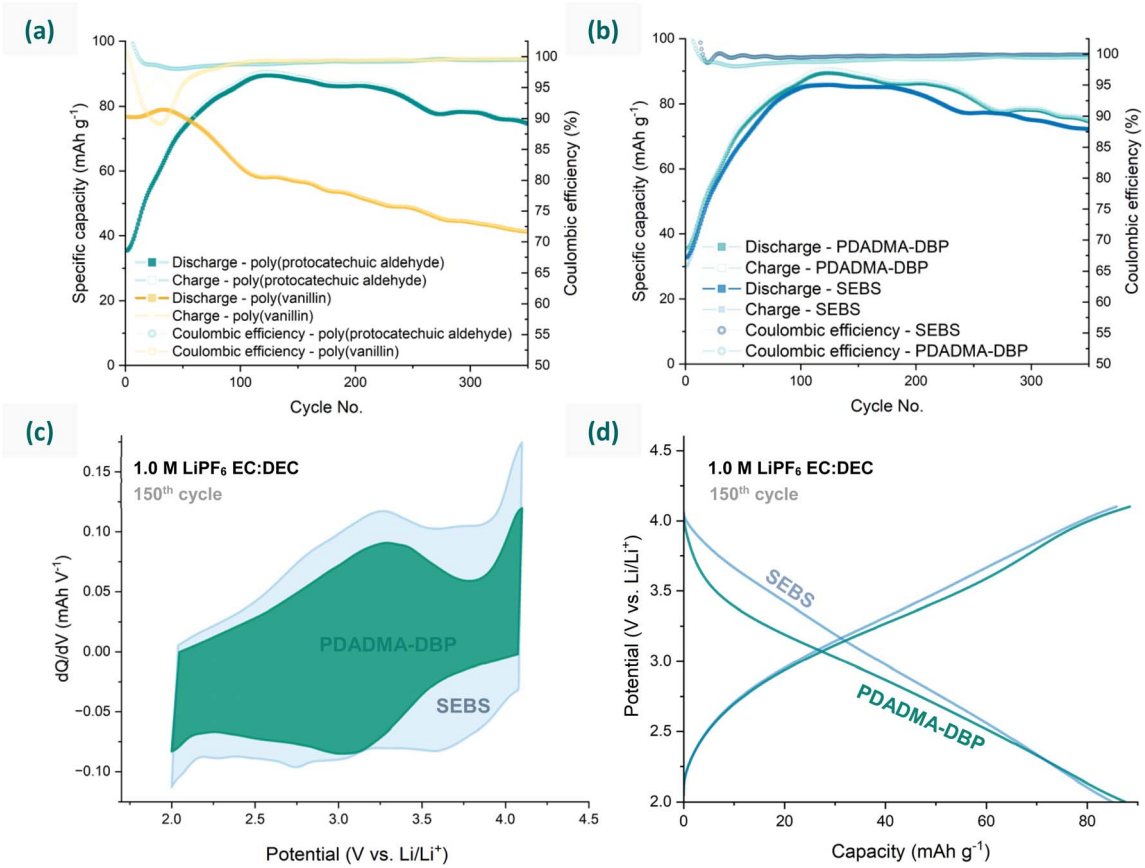


Fig. 3 (a) The charge and discharge capacity, as well as the correlated coulombic efficiency over 350 cycles for poly(vanillin) (green) and poly(protocatechuic aldehyde) (yellow) used as the cathode material in Li half-cells, utilizing [Act. Mat. : $C_{65}$ : PDADMA-DBP] = [40 : 50 : 10] as the electrode formulation and 1.0 M LiPF6 in EC : DEC (1 : 1, v/v) as the electrolyte with an applied C-rate of 0.1C. (b) The charge and discharge capacity, as well as the correlated coulombic efficiency over 350 cycles for poly(protocatechuic aldehyde) used as the cathode material in Li half-cells, utilizing [Act. Mat. : $C_{65}$ : binder] = [40 : 50 : 10] as the electrode formulation with 1.0 M LiPF6 in EC : DEC (1 : 1, v/v) as the electrolyte and an applied C-rate of 0.1C. Here, binder = SEBS or PDADMA-DBP. For the latter two cells, the comparison of (c) the d$Q$/d$V$ plot and (d) the voltage profile for the 150th cycle for both binders are also shown.

over 350 cycles for poly(protocatechuic aldehyde) with SEBS or PDADMA-DBP are shown. Interestingly, the PDADMA-DBP-based electrode slightly outperforms the one containing SEBS in terms of specific capacity at the peak value (90.68 *vs.* 86.14 mAh $g^{-1}$, respectively) and specific capacity after 350 cycles (respective 75.01 and 72.28 mAh $g^{-1}$). Moreover, the capacity retentions (82.7% and 83.9%) and coulombic efficiencies (99.49% and 99.93%) after 350 cycles as well as the activation phase show similar values for the two different battery designs. Indeed, another long activation phase of ≈130 cycles was observed, which is in agreement with earlier results displayed in Fig. 2a for the $LiPF_6$-based electrolyte. Possibly this is related to the combination of the electrolyte, polymer chemical structure and morphology, since any effect of the utilized binders can be excluded. Nonetheless, the results of the PDADMA-DBP-based electrode presented in Fig. 3b show that poly(protocatechuic aldehyde) performs well with the waterborne PDADMA-DBP binder, with comparable outcomes to the SEBS binder, paving the way towards the development of water soluble, sustainable bio-based organic electrodes.

In addition, the ionic nature of the PDADMA-DBP binder and intrinsic high ionic conductivity positively affect the electrochemical performance of the resulting organic electrodes, as can be noted from Fig. 3c and d. In Fig. 3c a comparison of the d$Q$/d$V$ plot for poly(protocatechuic aldehyde)-based electrodes with either SEBS or PDADMA-DBP as the binder is shown. The SEBS containing cell displays yet again a poor-defined catechol signal, where only a clear oxidation peak is visible. In contrast, the PDADMA-DBP containing cell shows a very clear oxidation and reduction signal at 3.2 V (*vs.* $Li/Li^+$) related to the catechol moiety. Consequently, the voltage profile improves significantly when moving from SEBS to PDADMA-DBP electrodes, as becomes clear from Fig. 3d.

## Conclusions

In this article, we show a green synthetic route to a vanillin bio-based redox polymer as a cathode material for lithium organic batteries. Two bio-based polymers, namely poly(vanillin) and poly(protocatechuic aldehyde), were synthesized as catechol-

bearing redox polymers. The synthesis was designed to be facile, scalable and quantitative, and solely makes use of the monomers, concentrated $H_2SO_4$ and water. In the case of vanillin, the polycondensation, demethylation and crosslinking occur simultaneously, delivering a catechol polymer derived from vanillin in one step. The ease of the process combined with the availability of especially bio-vanillin from biorefineries may allow for facile upscaling towards industrial production of bio-based poly(vanillin) cathode materials for batteries. Poly(protocatechuic aldehyde) containing a catechol redox moiety served as the reference polymer for the structural and electrochemical performance.

The electrochemical performance of both polymers was assessed as cathode materials in Li half-cells using different electrolytes. The best performance for poly(vanillin) as the cathode material in lithium metal/polymer cells showed peak specific capacities of 101.25 mAh $g^{-1}$, an improved capacity retention (85.5% *vs.* 72.1%, 280 cycles after the peak specific capacity) and a well-defined d$Q$/d$V$ plot showing a reversible catechol at 3.2 V (*vs.* Li/$Li^+$). Furthermore, the use of water to process the electrodes was showed using a poly(ionic liquid) binder. Interestingly, PDADMA-DBP with poly(protocatechuic aldehyde) and 1.0 M $LiPF_6$ in EC : DEC (1 : 1, v/v) showed the best electrochemical performance, outperforming its SEBS counterpart in terms of specific capacity (90.68 *vs.* 86.14 mAh $g^{-1}$, respectively), while displaying similar values for capacity retention and coulombic efficiency over 350 cycles. Values closer to the theoretical capacity value of the catechol redox polymer might be obtained by optimization attempts in future work. In summary, this work illustrates a scalable synthetic route to a bio-based catechol polymer from vanillin to be used as a high-voltage organic electrode material.

## Data availability

The ESI† can be requested from the editor and the metadata including ATR FTIR, $^1$H NMR, $^{13}$C solid-state NMR, cyclic voltammetry and galvanostatic cycling are available at a European-based repository.

## Author contributions

All authors contributed equally.

## Conflicts of interest

There are no conflicts to declare.

## Acknowledgements

The authors thank the European Union's Horizon 2020 research and innovation programme under the Marie Skłodowska-Curie Grant Agreement No. 860403 and No. 101028682 as well as the European Union's NextGenerationEU/PRTR programme. D. M. thanks Ayuda RYC2021-031668-IfinanciadaporMCIN/AEI/10.13039/501100011033 y por la Unión Europea NextGenerationEU/PRTR.

## Notes and references

1 M. Adsul, D. K. Tuli, P. K. Annamalai, D. Depan and S. Shankar, *Int. J. Polym. Sci.*, 2016, **2016**, 1857297.
2 M. R. Yates and C. Y. Barlow, *Resour., Conserv. Recycl.*, 2013, **78**, 54–66.
3 Z. Wang, M. S. Ganewatta and C. Tang, *Prog. Polym. Sci.*, 2020, **101**, 101197.
4 A. Llevot, E. Grau, S. Carlotti, S. Grelier and H. Cramail, *Macromol. Rapid Commun.*, 2016, **37**, 9–28.
5 F. Walch, O. Y. Abdelaziz, S. Meier, S. Bjelić, C. P. Hulteberg and A. Riisager, *Catal. Sci. Technol.*, 2021, **11**, 1843–1853.
6 J. Lora, Industrial Commrcial Lignins: sources, properteis and Applications, *Monomers, Polym. Compos. Renewable Resour.*, 2008, 225–241.
7 W. G. Glasser and S. S. Kelley, *Encyclopaedia of Polymer Science and Engineering*, 2nd edn, 1987.
8 F. G. Calvo-Flores and J. A. Dobado, *ChemSusChem*, 2010, **3**, 1227–1235.
9 J. Becker and C. Wittmann, *Biotechnol. Adv.*, 2019, **37**, 107360.
10 R. Hu, J. Zhan, Y. Zhao, X. Xu, G. Luo, J. Fan, J. H. Clark and S. Zhang, *Green Chem.*, 2023, **25**, 8970–9000.
11 D. Kai, M. J. Tan, P. L. Chee, Y. K. Chua, Y. L. Yap and X. J. Loh, *Green Chem.*, 2016, **18**, 1175–1200.
12 B. Jacobs, Y. Yao, I. Van Nieuwenhove, D. Sharma, G.-J. Graulus, K. Bernaerts and A. Verberckmoes, *Green Chem.*, 2023, **25**, 2042–2086.
13 C. Libretti, L. Santos Correa and M. A. R. Meier, *Green Chem.*, 2024, **26**, 4358–4386.
14 J. Zakzeski, P. C. A. Bruijnincx, A. L. Jongerius and B. M. Weckhuysen, *Chem. Rev.*, 2010, **110**, 3552–3599.
15 M. Kleinert and T. Barth, *Chem. Eng. Technol.*, 2008, **31**, 736–745.
16 M. Fache, B. Boutevin and S. Caillol, *Green Chem.*, 2016, **18**, 712–725.
17 S. Engelen, A. A. Wróblewska, K. De Bruycker, R. Aksakal, V. Ladmiral, S. Caillol and F. E. Du Prez, *Polym. Chem.*, 2022, **13**, 2665–2673.
18 M. Fache, A. Viola, R. Auvergne, B. Boutevin and S. Caillol, *Eur. Polym. J.*, 2015, **68**, 526–535.
19 M. Fache, R. Auvergne, B. Boutevin and S. Caillol, *Eur. Polym. J.*, 2015, **67**, 527–538.
20 L. Giraud, S. Grelier, E. Grau, L. Garel, G. Hadziioannou, B. Kauffmann, É. Cloutet, H. Cramail and C. Brochon, *Molecules*, 2022, **27**, 4138.
21 G. Garbay, L. Giraud, S. M. Gali, G. Hadziioannou, E. Grau, S. Grelier, E. Cloutet, H. Cramail and C. Brochon, *ACS Omega*, 2020, **5**, 5176–5181.
22 A. Llevot, E. Grau, S. Carlotti, S. Grelier and H. Cramail, *Polym. Chem.*, 2015, **6**, 6058–6066.
23 D. Breilly, S. Fadlallah, A. Flourat, P. Boustingorry, V. Froidevaux and F. Allais, *ACS Sustain. Chem. Eng.*, 2024, **12**, 10701–10712.
24 G. H. Ghuge, K. V. Kambikanam and K. S. Nair, *J. Appl. Polym. Sci.*, 2023, **140**, e54647.

 

25 S. K. Murthy, B. V. Basavaraj and B. Srinivasan, *Mater. Today: Proc.*, 2023, DOI: 10.1016/j.matpr.2022.12.227.
26 A. Navaruckiene, D. Bridziuviene, V. Raudoniene, E. Rainosalo and J. Ostrauskaite, *eXPRESS Polym. Lett.*, 2022, **16**, 279–295.
27 N. Fanjul-Mosteirín, L. P. Fonseca, A. P. Dove and H. Sardon, *Mater. Adv.*, 2023, **4**, 2437–2448.
28 M. Armand and J.-M. Tarascon, *Nature*, 2008, **451**, 652–657.
29 D. Larcher and J.-M. Tarascon, *Nat. Chem.*, 2015, **7**, 19–29.
30 M.-M. Titirici, *Adv. Energy Mater.*, 2021, **11**, 2003700.
31 P. Poizot, J. Gaubicher, S. Renault, L. Dubois, Y. Liang and Y. Yao, *Chem. Rev.*, 2020, **120**, 6490–6557.
32 N. Goujon, N. Casado, N. Patil, R. Marcilla and D. Mecerreyes, *Prog. Polym. Sci.*, 2021, **122**, 101449.
33 L. Liu, N. Solin and O. Inganäs, *Adv. Energy Mater.*, 2021, **11**, 2003713.
34 Y. Zhang, Z. Zhang, J. Jia, M. Yin, Z. He, H. Yu, Q. Zeng, D. Wang and X. Liu, *J. Electroanal. Chem.*, 2023, **932**, 117251.
35 C. Li, X. Liu, Z. He, W. Tao, Y. Zhang, Y. Zhang, Y. Jia, H. Yu, Q. Zeng, D. Wang, J. H. Xin, C. Duan and F. Huang, *J. Power Sources*, 2021, **511**, 230464.
36 W. Schlemmer, P. Nothdurft, A. Petzold, G. Riess, P. Frühwirt, M. Schmallegger, G. Gescheidt-Demner, R. Fischer, S. A. Freunberger, W. Kern and S. Spirk, *Angew. Chem., Int. Ed.*, 2020, **59**, 22943–22946.
37 A. Gallastegui, D. Minudri, N. Casado, N. Goujon, F. Ruipérez, N. Patil, C. Detrembleur, R. Marcilla and D. Mecerreyes, *Sustainable Energy Fuels*, 2020, **4**, 3934–3942.
38 N. Patil, A. Aqil, F. Ouhib, S. Admassie, O. Inganäs, C. Jérôme and C. Detrembleur, *Adv. Mater.*, 2017, **29**, 1703373.
39 T. Liu, K. C. Kim, B. Lee, Z. Chen, S. Noda, S. S. Jang and S. W. Lee, *Energy Environ. Sci.*, 2017, **10**, 205–215.
40 L. Dong, Y. Wang, Y. Dong, Y. Zhang, M. Pan, X. Liu, X. Gu, M. Antonietti and Z. Chen, *Nat. Commun.*, 2023, **14**, 4996.
41 I. K. Ilic, M. Meurer, S. Chaleawlert-umpon, M. Antonietti and C. Liedel, *RSC Adv.*, 2019, **9**, 4591–4598.
42 I. K. Ilic, K. Leus, J. Schmidt, J. Hwang, M. Maranska, S. Eigler and C. Liedel, *ACS Sustain. Chem. Eng.*, 2020, **8**, 3055–3064.
43 S. Zhang, Z. Gai, T. Gui, J. Chen, Q. Chen and Y. Li, *Evidence-Based Complementary Altern. Med.*, 2021, **2021**, 6139308.
44 A. C. Rolandi, C. Pozo-Gonzalo, I. de Meatza, N. Casado, D. Mecerreyes and M. Forsyth, *Adv. Energy Sustainability Res.*, 2023, **4**, 2300149.
45 F. M. Harth, B. Hočevar, T. R. Kozmelj, E. Jasiukaitytė-Grojzdek, J. Blüm, M. Fiedel, B. Likozar and M. Grilc, *Green Chem.*, 2023, **25**, 10117–10143.
46 M. Koyama, A. Takada and T. Ueda, *Chem. Pharm. Bull.*, 1982, **30**, 3239–3243.
47 D. S. Noyce and L. R. Snyder, *J. Am. Chem. Soc.*, 1959, **81**, 620–624.
48 S. Saito, T. Ohwada and K. Shudo, *J. Am. Chem. Soc.*, 1995, **117**, 11081–11084.
49 T. Lap, N. Goujon, D. Mantione, F. Ruipérez and D. Mecerreyes, *ACS Appl. Polym. Mater.*, 2023, **5**, 9128–9137.
50 K. Rehse and H.-G. Kawerau, *Arch. Pharm.*, 1974, **307**, 934–942.
51 W. Du, X. Du, M. Ma, S. Huang, X. Sun and L. Xiong, *Adv. Funct. Mater.*, 2022, **32**, 2110871.
52 B. C. Smith, *Spectroscopy*, 2022, **37**, 15–19.
53 V. Balachandran and K. Parimala, *Spectrochim. Acta, Part A*, 2012, **95**, 354–368.
54 I. A. Degen, *Appl. Spectrosc.*, 1968, **22**, 164–166.
55 L. Barbes, C. Radulescu and C. Stihi, *Rom. Rep. Phys.*, 2014, **66**, 765–777.
56 B. Peña, L.-C. de Ménorval, R. Garcia-Valls and T. Gumí, *ACS Appl. Mater. Interfaces*, 2011, **3**, 4420–4430.